Journal Pre-proofs

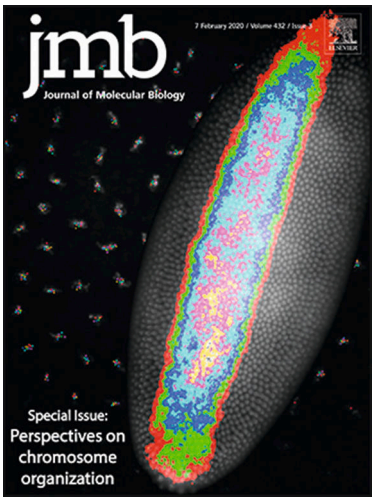

Brevia

Programmed flagellar ejection in *Caulobacter crescentus* leaves PL-subcomplexes

Mohammed Kaplan, Yuhang Wang, Georges Chreifi, Lujia Zhang, Yi-Wei Chang, Grant J Jensen

PII: S0022-2836(21)00205-9
DOI: https://doi.org/10.1016/j.jmb.2021.167004
Reference: YJMBI 167004

To appear in: *Journal of Molecular Biology*

Received Date: 11 December 2020
Revised Date: 12 April 2021
Accepted Date: 13 April 2021

Please cite this article as: M. Kaplan, Y. Wang, G. Chreifi, L. Zhang, Y-W. Chang, G.J. Jensen, Programmed flagellar ejection in *Caulobacter crescentus* leaves PL-subcomplexes, *Journal of Molecular Biology* (2021), doi: https://doi.org/10.1016/j.jmb.2021.167004

Programmed flagellar ejection in *Caulobacter crescentus* leaves PL-subcomplexes

Mohammed Kaplan[1], Yuhang Wang[1], Georges Chreifi[1], Lujia Zhang[2,3], Yi-Wei Chang[1,4] and Grant J Jensen[1,5,6]

[1]*Division of Biology and Biological Engineering, California Institute of Technology, Pasadena, CA 91125, USA*

[2]*Shanghai Engineering Research Center of Molecular Therapeutics and New Drug Development, School of Chemistry and Molecular Engineering, East China Normal University, Shanghai 200062, China*

[3]*New York University-East China Normal University Center for Computational Chemistry, New York University Shanghai, Shanghai 200062, China*

[4]*Present address: Department of Biochemistry and Biophysics, Perelman School of Medicine, University of Pennsylvania, Philadelphia, PA 19104, USA*

[5]*Department of Chemistry and Biochemistry, Brigham Young University, Provo, UT 84604, USA*

[6]*Corresponding author: Jensen@caltech.edu*

Abstract

The bacterial flagellum consists of a long extracellular filament that is rotated by a motor embedded in the cell envelope. While flagellar assembly has been extensively studied[1], the disassembly process remains less well understood. In addition to the programmed flagellar ejection that occurs during the life cycle of *Caulobacter crescentus*, we and others have recently shown that many bacterial species lose their flagella under starvation conditions, leaving relic structures in the outer membrane[2–7]. However, it remains unknown whether the programmed flagellar ejection of *C. crescentus* leaves similar relics or not. Here, we imaged the various stages of the *C. crescentus* life cycle using electron cryo-tomography (cryo-ET) and found that flagellar relic subcomplexes, akin to those produced in the starvation-induced process, remain as a result of flagellar ejection during cell development. This similarity suggests that the programmed flagellar ejection of *C. crescentus* might share a common evolutionary path with the more general, and likely more ancient[3], starvation-related flagellar loss.

The flagellar motor uses inner-membrane-embedded ion channels known as stators to generate torque, which is transferred from a cytoplasmic ring through a periplasmic driveshaft (the rod) and universal joint (the hook) to rotate the extracellular filament. Two rings act as bushings for the rod to pass through the cell wall (the P- (peptidoglycan) ring) and outer membrane (L- (lipopolysaccharide) ring). In addition, different periplasmic embellishing rings can surround the P- and L-rings in various species[8,9]. The assembly of this remarkable nanomachine has been studied extensively and seems to follow a conserved inside-out assembly pathway, starting from the inner-membrane-embedded components and proceeding outward[1].

On the other hand, flagellar disassembly has remained a largely unexamined terrain. Recently, we and others reported that many bacterial species lose their flagella in low-nutrient conditions, leaving a part of the motor, namely the P- and L-rings (termed the PL-subcomplex), as a relic in the outer membrane[2–5] (For a recent review see also Ref.[7]). Interestingly, this PL-subcomplex is plugged by a yet-unidentified protein, presumably to prevent the formation of a hole in the outer membrane. While this process was first reported in Gammaproteobacteria[2,4,5], it was later shown to be a widespread and ancient characteristic of the motor of many bacterial classes[3].

It has long been known that *C. crescentus* undergoes a programmed flagellar ejection during its developmental cycle[10]. This intricate cycle starts with a so-called "stalked cell" which is characterized by a long stalk at one of its poles. The stalk anchors the cell which divides asymmetrically to produce a motile "swarmer cell" which grows first a flagellum and then pili at the pole distal to the division site. Upon sensing and attaching to a new surface with its pili, the swarmer cell differentiates into a stalked cell, replacing its flagellum and pili with a stalk at the

same pole[10]. Interestingly, a previous study showed that ejected flagella isolated from an overnight culture of *C. crescentus* lack the PL-rings while purified hook-basal bodies retain them[11]. Also, while we previously reported the presence of PL-subcomplexes in poles of swarmer *C. crescentus*[3], it was unclear whether those subcomplexes were products of the life cycle or related to other reasons like starvation and mechanical stress.

Here, we imaged *C. crescentus* using cryo-ET (see supplementary Materials and Methods) and identified the various stages of its developmental cycle based on morphological features. While certain morphological features, like the presence of a stalk, are distinctive of certain stages in the lifecycle, others are more elusive. For example, it is difficult to determine whether a certain flagellar basal body is the result of a disassembly or assembly process. In our cryo-tomograms, we identified the following stages: ***i***) flagellated poles without pili (**Fig. 1A**); ***ii***) poles with flagella and pili (**Fig. 1B**); ***iii***) poles with pili and flagellar basal bodies (motors without the extracellular hook or filament), suggesting a recent ejection event as flagella are built before pili[10] (**Fig. 1C**); ***iv***) poles with pili, PL-subcomplexes and budding stalks (**Fig. 1D**); and ***v***) poles with PL-subcomplexes and stalks of various lengths (examples shown in **Fig. 1E-I**). The presence of the PL-subcomplex on stalked poles, either on the stalk itself (**Fig. 1F- H**) or in its vicinity (**Fig. 1I**), indicates that this programmed process of ejection leaves relics similar to those from the starvation-related process.

By performing subtomogram averaging on the identified PL-subcomplexes, we found that they contain, in addition to the P- and L-rings, two other periplasmic rings known as the outer membrane (OM) ring and the cogwheel (**Fig. 1J**), which are also present in the fully-assembled

motor of *C. crescentus*[12]. These two rings were not visible in the PL-subcomplex previously reported on the poles of swarmer cells due to the low number of particles identified at the time[3]. Interestingly, while there is a hole in the S-layer through which the hooks of fully-assembled flagella penetrate to the exterior of the cell, the S-layer appeared continuous above the PL-subcomplexes (Fig. S1).

To confirm that the observed PL-subcomplexes are related to the programmed ejection process and not only due to starvation or mechanical stress, we imaged a strain lacking the response regulator PleD (*C. crescentus* D*pleD*), which is responsible for efficient flagellar ejection during the developmental lifecycle[13]. We prepared two samples of *C. crescentus* D*pleD* grown to different OD_{600} levels, these being: low OD_{600} ~0.5-0.6 and high OD_{600} ~2, referred to henceforth as LOD and HOD respectively. The LOD sample has a similar OD_{600} to that of cells where PL-subcomplexes were first identified (Fig. 1), while the HOD is expected to have more starvation-related PL-subcomplexes as previously shown[2,4,14]. This allowed us to compare the number of PL-subcomplexes in cells which either do (wildtype) or do not (D*pleD* cells) undergo programmed flagellar ejection (see Materials and Methods).

In the cryo-tomograms of *C. crescentus* D*pleD* cells, the flagella were still present on stalked poles due to the inability of these cells to eject their flagella during their development cycle (Fig. 2A). Occasionally, flagellar basal bodies were also seen on the stalks (Fig. 2B). The number of PL-subcomplexes in the cryo-tomograms of *C. crescentus* D*pleD* cells was significantly lower than on wildtype cells (Fig. 2 C&D and Table 1). While we observed PL-subcomplexes on almost all the stalked poles of wildtype *C. crescentus*, only 6% of HOD D*pleD* stalks had PL-subcomplexes

that we could identify (Fig. 2C and Table 1), and in LOD D*pleD* cells, only one PL-subcomplex was identified. The latter was identified in a lysed cell (Fig. 2D), and the inner membrane subcomplex (consisting of the cytoplasmic (C-) ring and the membrane/supramembrane (MS-) ring) was also present near it, similar to what was previously seen in *Legionella pneumophila* and *Campylobacter jejuni*[2,3]. PL-subcomplexes were also observed on non-stalked poles of wildtype cells. At first it was unclear whether these were cells frozen in the moments between programmed flagellar ejection and stalk development, or some other process. While ~10% of wildtype cells exhibited PL-subcomplexes on non-stalked poles (18/201), only 1 PL-subcomplex was observed on a non-stalked pole in all 259 D*pleD* cells. Thus the PL-subcomplexes seen on non-stalked poles of wildtype cells were also the result of programmed flagellum ejection, rather than some other processes (like starvation or mechanical stress). In total 35 PL-subcomplexes were observed on 201 wildtype cells, and only 3 were seen on 259 D*pleD* cells. This strong correlation between the ability of *C. crecentus* to eject its flagellum during its life cycle and the presence of PL-subcomplexes indicate that the vast majority of the observed PL-subcomplexes are related to the programmed ejection process.

The fact that the programmed flagellar ejection process associated with the *C. crescentus* life cycle leaves plugged PL-subcomplexes similar to those seen in nutrient-deprived cells suggests that the two processes are evolutionarily linked. It is plausible that the specialized flagellar loss occurring during *C. crescentus* differentiation evolved from a general and more ancient mechanism associated with starvation, a hypothesis that is bolstered by the fact that *C. crescentus* has evolved to inhabit low-nutrient aquatic environments[10]. This connection between the two phenomena might yield useful clues from the considerable body of literature on *C. crescentus* flagellar ejection that

could help us decipher the potential and yet-unknown signal transduction pathway(s) associated with starvation-related flagellar loss[14].

References:

1. Macnab, R.M. (2003). How Bacteria Assemble Flagella. Annual Review of Microbiology *57*, 77–100.

2. Kaplan, M., Subramanian, P., Ghosal, D., Oikonomou, C.M., Pirbadian, S., Starwalt-Lee, R., Mageswaran, S.K., Ortega, D.R., Gralnick, J.A., El-Naggar, M.Y., et al. (2019). *In situ* imaging of the bacterial flagellar motor disassembly and assembly processes. The EMBO Journal, e100957.

3. Kaplan, M., Sweredoski, M.J., Rodrigues, J.P.G.L.M., Tocheva, E.I., Chang, Y.-W., Ortega, D.R., Beeby, M., and Jensen, G.J. (2020). Bacterial flagellar motor PL-ring disassembly subcomplexes are widespread and ancient. Proceedings of the National Academy of Sciences, 201916935.

4. Ferreira, J.L., Gao, F.Z., Rossmann, F.M., Nans, A., Brenzinger, S., Hosseini, R., Wilson, A., Briegel, A., Thormann, K.M., Rosenthal, P.B., et al. (2019). γ-proteobacteria eject their polar flagella under nutrient depletion, retaining flagellar motor relic structures. PLOS Biology *17*, e3000165.

5. Zhu, S., Schniederberend, M., Zhitnitsky, D., Jain, R., Galán, J.E., Kazmierczak, B.I., and Liu, J. (2019). *In Situ* Structures of Polar and Lateral Flagella Revealed by Cryo-Electron Tomography. Journal of Bacteriology *201*.

6. Zhuang, X., Guo, S., Li, Z., Zhao, Z., Kojima, S., Homma, M., Wang, P., Lo, C., and Bai, F. (2020). Live-cell fluorescence imaging reveals dynamic production and loss of bacterial flagella. Molecular Microbiology *114*, 279–291.

7. Zhuang, X.-Y., and Lo, C.-J. (2020). Construction and Loss of Bacterial Flagellar Filaments. Biomolecules *10*, 1528.

8. Chen, S., Beeby, M., Murphy, G.E., Leadbetter, J.R., Hendrixson, D.R., Briegel, A., Li, Z., Shi, J., Tocheva, E.I., Müller, A., et al. (2011). Structural diversity of bacterial flagellar motors: Structural diversity of bacterial flagellar motors. The EMBO Journal *30*, 2972–2981.

9. Kaplan, M., Ghosal, D., Subramanian, P., Oikonomou, C.M., Kjaer, A., Pirbadian, S., Ortega, D.R., Briegel, A., El-Naggar, M.Y., and Jensen, G.J. (2019). The presence and absence of periplasmic rings in bacterial flagellar motors correlates with stator type. eLife *8*.

10. Curtis, P.D., and Brun, Y.V. (2010). Getting in the Loop: Regulation of Development in Caulobacter crescentus. Microbiology and Molecular Biology Reviews *74*, 13–41.

11. Kanbe, M. (2005). Protease susceptibility of the Caulobacter crescentus flagellar hook-basal body: a possible mechanism of flagellar ejection during cell differentiation. Microbiology *151*, 433–438.

12. Rossmann, F.M., Hug, I., Sangermani, M., Jenal, U., and Beeby, M. (2020). In situ structure of the *Caulobacter crescentus* flagellar motor and visualization of binding of a CheY-homolog. Molecular Microbiology *114*, 443–453.

13. Aldridge, P., and Jenal, U. (1999). Cell cycle-dependent degradation of a flagellar motor component requires a novel-type response regulator. Molecular Microbiology *32*, 379–391.

14. Zhu, S., and Gao, B. (2020). Bacterial Flagella Loss under Starvation. Trends in Microbiology.

15. Schrader, J.M., and Shapiro, L. (2015). Synchronization of Caulobacter Crescentus for Investigation of the Bacterial Cell Cycle. Journal of Visualized Experiments.

16. Chreifi, G., Chen, S., Metskas, L.A., Kaplan, M., and Jensen, G.J. (2019). Rapid tilt-series acquisition for electron cryotomography. Journal of Structural Biology *205*, 163–169.

17. Eisenstein, F., Danev, R., and Pilhofer, M. (2019). Improved applicability and robustness of fast cryo-electron tomography data acquisition. Journal of Structural Biology *208*, 107–114.

18. Chreifi, G., Chen, S., and Jensen, G.J. (2021). Rapid tilt-series method for cryo-electron tomography: Characterizing stage behavior during FISE acquisition. Journal of Structural Biology *213*, 107716.

19. Mastronarde, D.N. (2005). Automated electron microscope tomography using robust prediction of specimen movements. J. Struct. Biol. *152*, 36–51.

20. Hagen, W.J.H., Wan, W., and Briggs, J.A.G. (2017). Implementation of a cryo-electron tomography tilt-scheme optimized for high resolution subtomogram averaging. J. Struct. Biol. *197*, 191–198.

21. Kremer, J.R., Mastronarde, D.N., and McIntosh, J.R. (1996). Computer visualization of three-dimensional image data using IMOD. J. Struct. Biol. *116*, 71–76.

Figures:

Figure 1

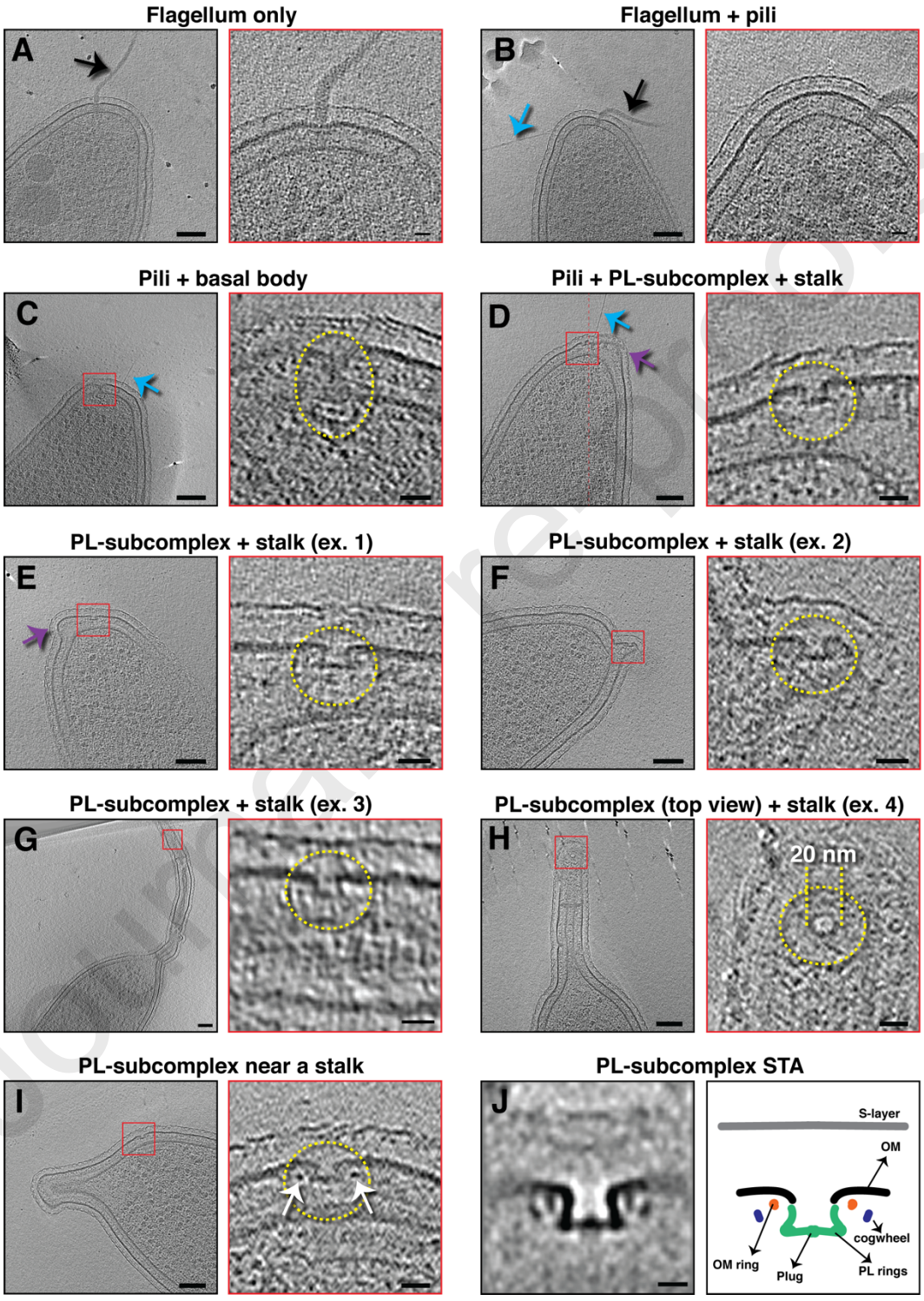

Figure 2

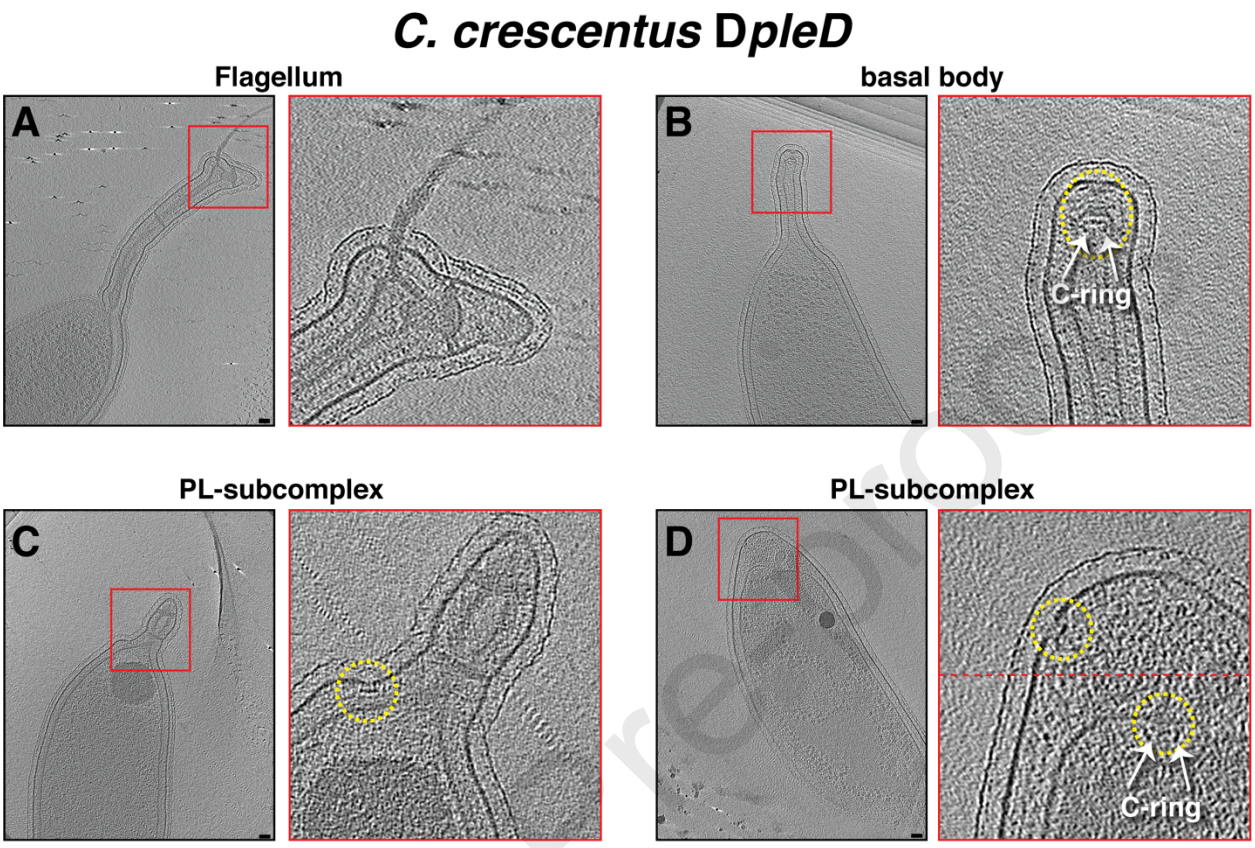

TABLE 1

	Total no. of tomograms	Total no. of stalks in tomograms	PL-subcomplexes on stalked poles	PL-subcomplexes on non-stalked poles
C. crescentus	201	18	17	18
C. crescentus D*pleD* (LOD)	159	41	0	1 (lysed)
C. crescentus D*pleD* (HOD)	100	29	2	0

Figure legends:

Figure 1: A-I) slices through electron cryo-tomograms of *C. crescentus* cells in various stages of the life cycle, described in the text. Red bordered panels contain enlarged views of the boxed areas. Black arrows point to flagella, light blue arrows to pili, purple arrows to budding stalks, and white arrows to the cogwheel. Dashed yellow circles highlight PL-subcomplexes, and the dashed ellipse in (C) highlights a flagellar basal body. (E-H) depict multiple examples (ex.) of PL-subcomplexes located on stalks of different lengths. The vertical dashed red line in (D) indicates a composite of two images with different z-heights from the same tomogram. Scale bars are 100 nm (black-bordered panels) and 20 nm (red-bordered panels).

J) a central slice through the subtomogram average (STA) of the PL-subcomplex, with features annotated on the right. Scale bar is 10 nm.

Figure 2: A-C) slices through electron cryo-tomograms of *C. crescentus* D*pleD* cells showing the presence of a flagellum (A), a basal body (B) and a PL-subcomplexes (C) on the stalks. **D)** a slice through electron cryo-tomogram of a lysed LOD *C. crescentus* D*pleD* highlighting the presence of a PL-subcomplex and an inner-membrane subcomplex (white arrows point to the C-ring). Red bordered panels contain enlarged views of the boxed areas. The vertical dashed red line in (D) indicates a composite of two images with different z-heights from the same tomogram. Dashed yellow circles highlight PL-subcomplexes in (C&D) and the inner membrane subcomplex in (D), while dashed yellow ellipse in (B) highlights the basal body. Scale bars are 50 nm

Supplementary Figures:

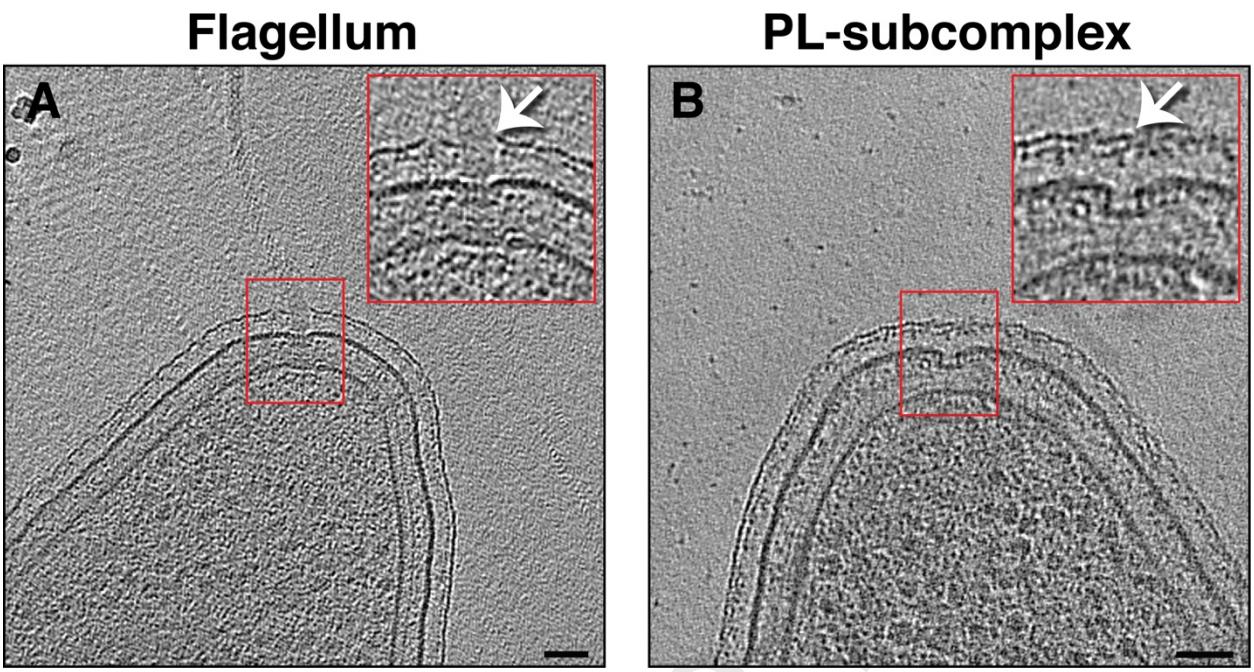

Figure S1: slices through electron cryo-tomograms of *C. crescentus* with a flagellum (A) and a PL-subcomplex (B) indicating the presence of a hole in the S-layer in (A, white arrow) and a continuous S-layer above the PL-subcomplex (B, white arrow). Red bordered panels contain enlarged views of the boxed areas. Scale bars are 50 nm.

Supplementary Materials and Methods:

Growth conditions

M2G and M2 media for culturing *Caulobacter crescentus* were prepared according to a previously published protocol[15]. 5 mL of M2G media were inoculated with a frozen stock of *C. crescentus* NA 1000 and grown overnight at 28 ℃. Subsequently, 5 mL of the overnight culture was diluted in 15 mL M2G and grown at 28 ℃ with a shaking speed of 200 rpm for ~2 hours until mid-log phase (OD_{600} 0.4-0.5). The sample was then centrifuged at 5200 x g for 6 minutes at 4 ℃ (same temperature for all subsequent centrifugation steps) and the pellet was resuspended in 1 mL M2 solution. The resuspended cells were transferred into a 2-mL microcentrifuge tube and centrifuged at 5200 x g for 5 minutes. All but ~250 µL of supernatant was removed, 650 µL M2 was added and the pellet was resuspended. 900 µL cold Percoll (Sigma Aldrich) was added and the sample was centrifuged at 15,000 x g for 20 minutes. The stalked cells will be near the surface of the solution while swarmer cells near the bottom. Note that both wild-type cells and cells that lack CapF protein (a protein related to the TAD pilus and which we imaged for the aim of studying this pilus system, and both of these strains were supplied from the lab of Prof. Patrick Viollier from the University of Geneva) were both grown using this protocol. Both of them were considered as cells that are capable of ejecting their flagella in a programmed way and were combined together in the statistical analysis shown in Table 1.

C. crescentus D*pleD* cells (strain UJ4450, supplied by the lab of Prof. Urs Jenal from the University of Basel) were grown in PYE medium at 30° C with shaking at 220 rpm. For the LOD sample (OD_{600} ~ 0.5-0.6), cells were grown for ~ 10 hours from a glycerol stock, while the HOD cells (OD_{600} ~ 2) were grown overnight. Cells were spun down at 5000 rpm for 3 minutes and

concentrated ten times and then mixed with 10 nm gold nanoparticles. Subsequently, 4 µL of this mixture was applied to glow-discharged, carbon-coated, R2/2, 200 mesh gold Quantifoil grids (Quantifoil Micro Tools) in a Vitrobot chamber (FEI) and excess fluid was blotted away prior to plunge-freezing.

Cryo-ET sample preparation, data collection and processing:

Data acquisition and analysis for cells capable of ejecting their flagella were performed as described in reference[3]. Data was collected with a pixel size of 3.51 Å and a cumulative electron dose of ~180 $e^-/Å^2$. In total, 22 particles were averaged, with twofold symmetrization along the particle *y*-axis applied.

C. crescentus D*pleD* data was acquired on a Titan Krios cryo-TEM (Thermo Fisher Scientific) equipped with a Gatan energy filter and K3 direct electron detector (Gatan) operating in counting mode and correlated double-sampling mode. Tilt-series were acquired using the fast-incremental single exposure (FISE) method as previously developed[16–18] in serialEM software[19], using a grouped dose-symmetric tilt scheme[20], a tilt range of -60° to +60°, 3° tilt increment, target defocus of -8 µm, pixel size of 4.49Å/pixel, frame time of 0.05 sec/frame, and a total dose of 180 $e^-/Å^2$. FISE tilt-series were gain normalized and motion-corrected using IMOD's alignframes[21].

Acknowledgments:

This project was funded by the NIH (grant R35 GM122588 to G.J.J.) and a Baxter postdoctoral fellowship from Caltech to M.K. Cryo-ET work was done in the Beckman Institute Resource Center for Transmission Electron Microscopy at the California Institute of Technology. We are

grateful to Catherine Oikonomou for critically reading the manuscript. We thank Ariane Briegel for collecting some of the data and Songye Chen for technical support. We are grateful to the lab of Prof. Patrick Viollier (University of Geneva) for sending wild type and delta CapF strains. The *C. crescentus* D*pleD* strain (UJ4450) was kindly sent to us from the lab of Prof. Urs Jenal (University of Basel), and we also thank Prof. Urs Jenal for critically reading our manuscript.

Highlights

- Imaging the swarmer-to-stalked transition in *Caulobacter crescentus* using cryo-ET.
- The programmed flagellar ejection leaves flagellar PL-subcomplexes on the stalks.
- These relics are similar to those produced in the starvation-induced flagellar loss.
- This suggests an evolutionary connection between these two phenomena.

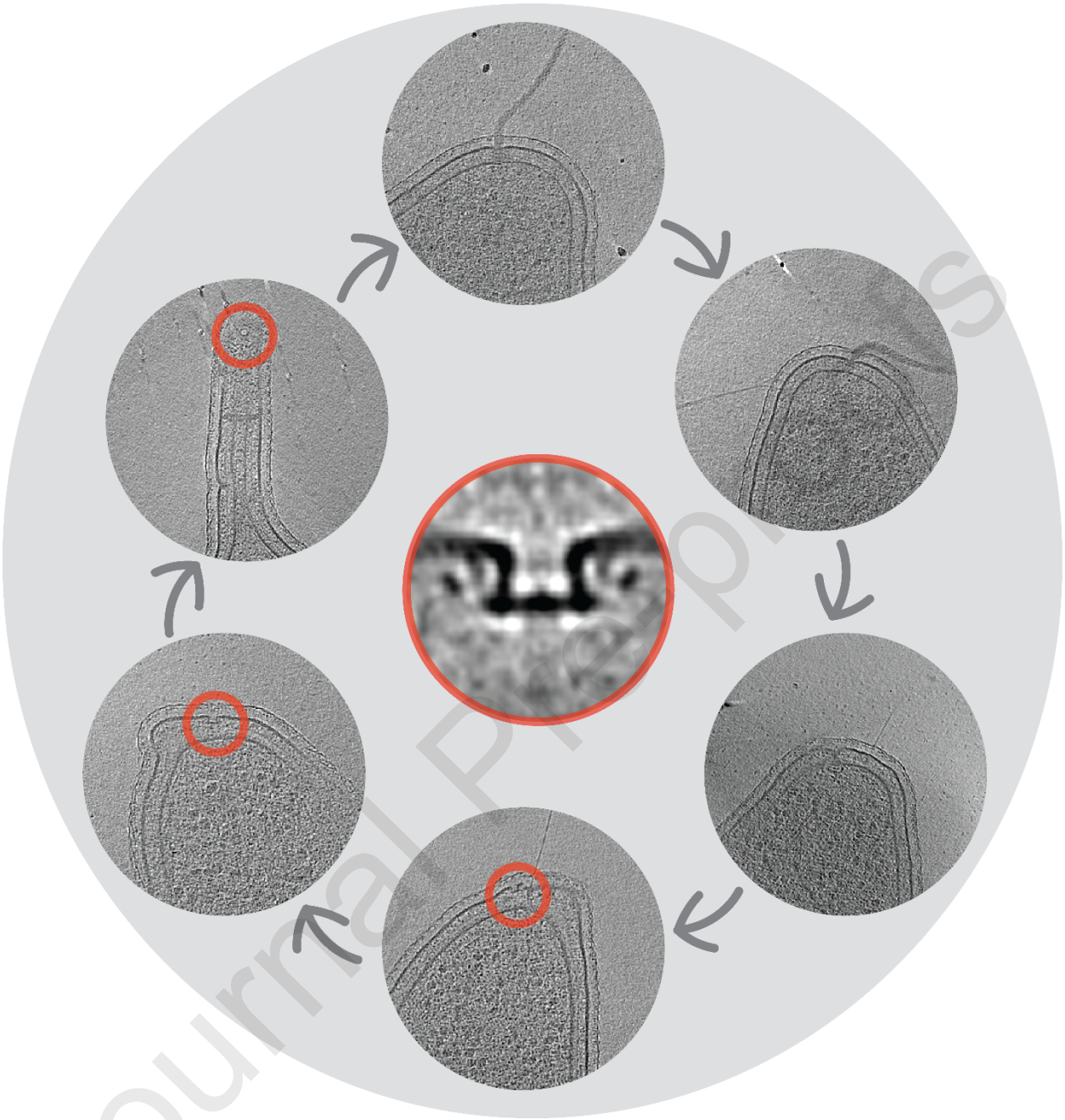

Declaration of interests

☒ The authors declare that they have no known competing financial interests or personal relationships that could have appeared to influence the work reported in this paper.

☐The authors declare the following financial interests/personal relationships which may be considered as potential competing interests:

Mohammed Kaplan: Conceptualization, Data collection, Data analysis, writing original draft and editing, Funding acquisition.

Yuhan Wang: Data collection and Writing-review and editing.

Georges Chreifi: Data collection and Writing-review and editing.

Lujia Zhang: Data collection and Writing-review and editing.

Yi-Wei Chang: Data collection and Writing-review and editing.

Grant J Jensen: Conceptualization, Data analysis, Writing-review and editing, Funding acquisition.